A Comparison of Rib Structural and Material Properties from Matched Whole Rib Bending and Tension Coupon Tests

Devon L. Albert, Yun-Seok Kang, Amanda M. Agnew, Andrew R. Kemper

Abstract The chest is one of the most frequently injured body regions in motor vehicle collisions. However, the relationship between the structural and material properties of the ribs has been largely unstudied. Therefore, the purpose of this study was to evaluate potential correlations between the structural properties of whole ribs and the material properties of rib cortical bone. Twenty-nine pairs of sixth ribs underwent whole rib bending tests and coupon tension tests to quantify the structural and material properties, respectively. Analogous material and structural properties were paired, and both parametric and non-parametric measures of correlation were calculated. For each pair, the percent variance of the structural property explained by the material property was assessed by calculating R^2 values. All pairs resulted in positive correlations. A significant correlation indicated that the material property influenced the structural property. However, all pairs, including those with significant correlations, had R^2 values below 0.5, indicating the material properties did not explain the majority of the variance of the structural properties. Overall, this study is the first step toward determining the relative contributions of material properties on the structural response of whole ribs.

Keywords Cortical bone, thorax injury, modulus, stiffness, strain energy density, total energy

I. INTRODUCTION

The chest is the second most injured body region in motor vehicle collisions, contributing to approximately 65% of all blunt chest trauma [1][2]. Variation in thoracic injury tolerance between individuals has been attributed to variation in age, gross rib geometry, cross-sectional geometry, and material properties [3-7]. Although, several studies have investigated rib structural properties [6-16] and rib cortical bone material properties [7][17-19], few studies have attempted to investigate the relationship between the structural and material properties. Kemper *et al.* [7] conducted matched 3-point bending tests and coupon tension tests at different regions along the rib and at different rib levels in order to determine whether variation in material properties contributed to the within subject variation observed in the structural response of the rib. No significant difference in material properties was observed across rib region or level, while variation in the structural properties were attributed to variation in rib cross-sectional geometry. However, the structural testing was performed on relatively straight whole rib sections, as opposed to the entire rib. Therefore, the structural responses obtained cannot be extrapolated to the structural response of the whole rib, which encompasses more complex geometries. Additionally, the study did not assess the degree of correlation between the measured material and structural properties.

Further research is necessary to link the structural response of the whole rib to the material properties of the rib cortical bone in order to assess the relative contributions of material properties and geometry on thoracic injury tolerance. Therefore, the purpose of this study was to evaluate potential correlations between the structural and material properties of the rib for both sexes over a wide range of ages by performing matched whole rib bending tests and coupon tension tests.

II. METHODS

Paired sixth ribs from 29 individuals (16 male, 13 female), ranging from 24 to 99 years of age (mean: 67.6 ± 20.5 years), were included in this study. The ribs were ethically obtained through the Body Donation Program at

D. L. Albert is a PhD student in Biomedical Engineering at Virginia Tech in Blacksburg, VA, USA (email: dla16@vt.edu). Y. S. Kang and A. M. Agnew are affiliated with the Injury Biomechanics Research Center (IBRC) at the Ohio State University, Columbus, OH, USA. D. L. Albert and A. R. Kemper are affiliated with the Center for Injury Biomechanics (CIB) at Virginia Tech.

The Ohio State University and Lifeline of Ohio. The full length of the left and right ribs was excised from each donor soon after the time of death, wrapped in saline soaked gauze, stored in plastic bags, and frozen to a temperature of -20°C until testing so that the material properties of the bone would not be altered [20-24]. The left or right rib was randomly selected to undergo a whole rib bending test to quantify the structural properties, while the contralateral rib was selected for coupon tension tests to quantify the material properties. It was assumed that the material properties would be consistent between matched left and right ribs because Kemper *et al.* [7][17] observed no significant differences in rib material properties with respect to rib region (anterior, lateral, and posterior) or rib level within the same subject. Before both types of testing, the ribs were thawed, and the soft tissue was removed. Specimens were kept hydrated with saline during both the preparation and experimental phases of both the bending and tension tests.

Whole Rib Bending Tests

The whole rib anterior/posterior bending tests were conducted using a custom pendulum fixture, as described in [6] and [25], that was designed to simulate a frontal thoracic impact (Figure 1). The pendulum impacted the ribs at approximately 2 m/s, causing the sternal end of the rib to translate toward the fixed vertebral end. This produced a strain rate of approximately 0.5 strain/s. The ribs were instrumented with four uniaxial strain gages applied to the pleural and cutaneous surfaces at approximately 30% and 60% of the rib curve length from the vertebral end. The test fixture was instrumented with a 6-axis reaction load cell (CRABI neck load cell, IF-954, Humanetics, Plymouth, MI) to measure forces and moments. The linear displacement of the sternal end of the rib was measured using a string potentiometer (Rayelco P-20A, AMETEK, Inc., Berwyn, PA). The forces and linear displacements were filtered using SAE channel filter class (CFC) 180 [26]. The peak force was defined as the maximum force in the direction of impact as measured from the reaction load cell. It should be noted that this value cannot be assumed to be constant along the length of the rib. The maximum percent linear displacement was calculated as a percentage of the total span length. Linear structural stiffness was calculated as the slope of 20–80% of the elastic portion of the force-displacement curve as described in [6]. The total energy was defined as the area under the force-displacement curve until the time of fracture. High speed video (Phantom, Vision Research, Inc., Fort Wayne, IN) of the bending tests was collected at 1000 frames/s.

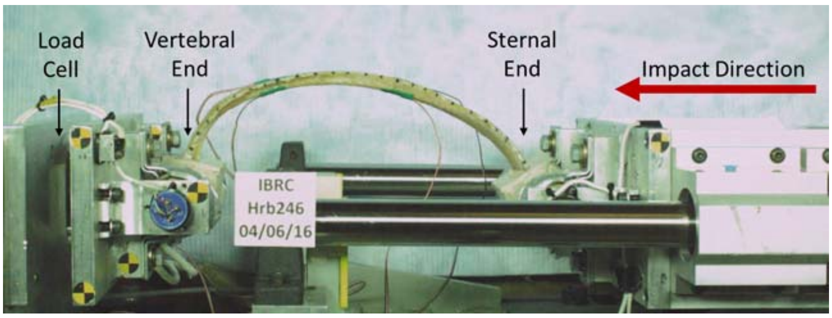

Fig. 1. Whole rib bending test setup.

Coupon Tension Tests

Cortical bone tension coupons were fabricated from the ribs contralateral to those used in the whole rib bending tests and were tested to failure in tension according to the methodology presented in [7] and [17]. In brief, rectangular sections (30 mm long and 9 mm wide) of the cutaneous cortical bone were cut using a custom-made low-speed circular saw with a diamond encrusted blade. The rectangular sections were aligned with the main axis of the rib and were cut from the anterior or lateral aspect of the rib. In two separate studies, Kemper *et al*. found no significant difference in material properties between the anterior, lateral, and posterior aspects of the rib [7][17]. Therefore, coupons were obtained from the location along the rib with sufficient width and the least amount of natural curvature, regardless of the anatomical region. Because the posterior aspect has a higher curvature than the rest of the rib, samples were only taken from the anterior and lateral aspects. In the event that the rib was too narrow to obtain a sample with the correct width, the sample was cut to the maximum width possible. Decreasing grits of sand paper (240, 320, 400, and 600) were used to sand both sides of the specimen until the sample thickness was uniform within 0.127 mm. Then, the sample was milled into a dog-bone shape using a Computer Numerical Control (CNC) mill (MAXNC 10, Ximotion LLP, Gilbert, AZ)

(Figure 2). After the milling process was completed, samples were sanded to their final thicknesses, which was uniform within 0.0254 mm. The thicknesses and widths of the gage length of each sample were measured with calipers in order to calculate stress during the tensile tests.

Uniaxial tensile tests were performed on a high-rate servo-hydraulic Material Testing System (810 MTS, MTS, Eden Prairie, MN) using custom designed coupon grips and a slack adapter (Figure 3). The custom slack adapter was used to ensure that the coupons experienced a constant strain rate throughout the entire test. Care was taken to confirm the alignment of the top and bottom grips so that the coupons were experiencing a purely tensile load [17]. Coupons were pulled in tension past the point of failure at a target strain rate of 0.5 strain/s. Data from the uniaxial load cell (1500ASK-100, Interface, Scottsdale, AZ) and extensometer (632.13F-20, MTS, Eden Prairie, MN) were collected at 40100.2 Hz and filtered at SAE CFC 180 [26]. Strain was calculated from the extensometer output by dividing the change in length between the extensometer arms by the initial length between the arms. Stress was calculated by dividing the force by the initial cross-sectional area of the coupon gage length. The yield point was calculated as the point of intersection between the stress-strain curve and a straight line at a 0.2% strain offset that was parallel to the elastic portion of the curve. The elastic modulus was calculated as the slope between two points on the stress-strain curve that were approximately 30% and 70% of the yield point. The failure stress and failure strain were defined as the stress and strain at the time of failure. Lastly, the strain energy density was calculated as the integral of the stress-strain curve. Failure stress, failure strain, and strain energy density could not be determined for coupons that failed outside of the extensometer arms (n = 10). Therefore, only the elastic modulus was included in the data analysis for these tests. If the coupon failed outside of the extensometer arms, a replacement coupon was fabricated from the same rib and tested. However, only one repeat test was performed per subject. This resulted in a total of 37 tests.

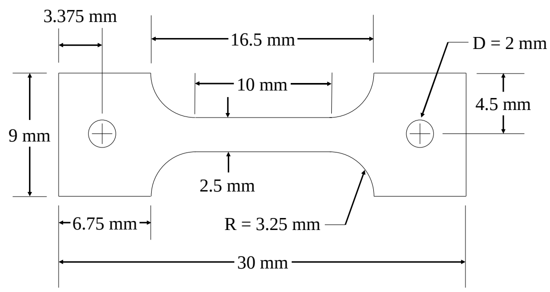

Fig. 2. Coupon schematic.

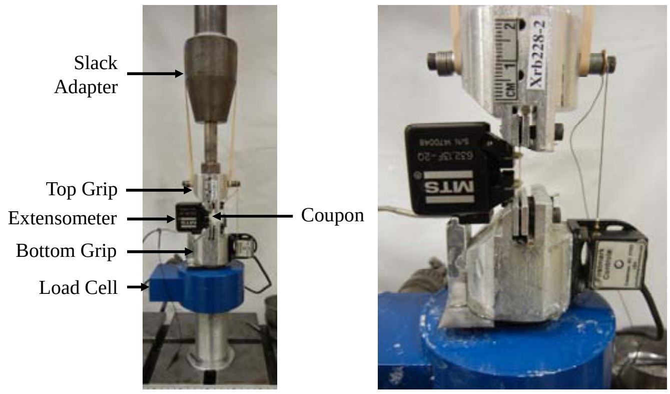

Fig. 3. Coupon tensile test setup.

Statistical Analysis

The degree of linear correlation between analogous pairs of material and structural properties from the coupon and bending tests, respectively, was statistically assessed. The comparisons were made between pairs of material and structural parameters that represented similar properties including compliance (e.g. modulus vs stiffness), displacement (e.g. failure strain vs linear displacement), force (e.g. failure stress vs peak force), and energy (e.g. strain energy density vs total energy). The pairs included the coupon elastic modulus and whole rib stiffness, coupon failure strain and whole rib linear displacement, coupon failure strain and whole rib peak tensile strain, coupon failure stress and whole rib peak force, and coupon strain energy density and whole rib total energy. All properties were tested for normality using a Shapiro-Wilk test. At least one property was not normally distributed. Therefore, the non-parametric Spearman's rank correlation coefficient (ρ) was determined for each pair in addition to the Pearson correlation coefficient (r), which assumes normality. The statistical significance of each test statistic was calculated using a Students t-test. Significance was ascertained using an alpha level of 0.05 for all analyses. The coefficient of determination (R^2) was also calculated for each comparison based on a linear regression in order to assess the percent variance of the structural property explained by the material property.

III. RESULTS

During the bending tests, translation of the sternal end of the rib toward the vertebral end resulted in increased rib curvature (Figure 4). The cutaneous cortex of the rib experienced tensile loading, while the pleural cortex experienced compressive loading. The ribs were loaded to failure, resulting in one or two fractures. Ribs with two fractures experienced both fractures almost simultaneously as their times of fracture could not be distinguished using the high speed video. Fracture location varied between specimens, but fractures mostly occurred in the anterior and lateral regions of the rib. It was not always possible to confirm that fracture initiated on the cutaneous (tensile) surface of the rib during the bending tests using the high speed video due to the rapidity of the event. However, a previous study using the same experimental setup was able to confirm that fracture initiated on the tensile surface for all tested ribs and provided a more complete description of fracture mechanisms [8].

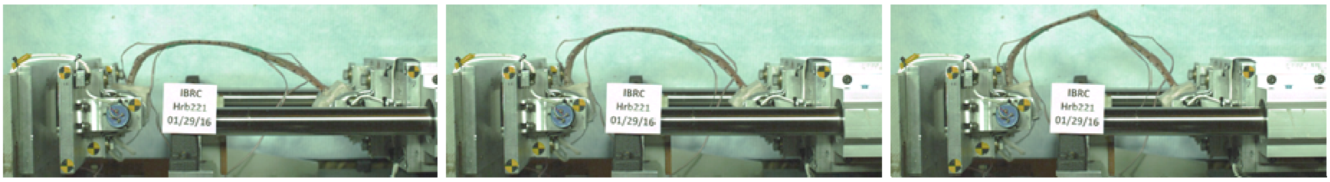

Fig. 4. Video stills from a bending test with the rib in the initial position (left), displaced before fracture (middle), and during fracture (right).

In order to determine whether the cutaneous cortex of the rib in the bending tests and the coupons in the tensile tests experienced comparable loading, the strain rates and direction of principal strain were compared. The average strain rates from the bending and coupon tests were 0.522 and 0.516 strain/s, respectively. Additionally, an analysis of principal strains for one rib instrumented with rosette strain gages during a bending test showed that the maximum principal strain was within 10 degrees of the main axis of the rib. This coincides with the coupon tests since the coupons were fabricated to align with the main axis of the rib. Therefore, the cortical bone experienced similar loading in both the bending and coupon tests.

Analogous structural properties and material properties from the bending tests and coupon tests, respectively, were plotted in Figure 5. The means of the structural and material properties are presented in Table I. The structural properties of linear displacement ($W = 0.8287$, $p < 0.0001$), peak tensile strain ($W = 0.9224$, $p = 0.0148$), and total energy ($W = 0.8072$, $p = 0.0025$) were not found to be normally distributed. This prompted a non-parametric analysis of correlation (Spearman correlation) in addition to the Pearson correlation for the material-structural property pairs that were normally distributed. The results of both analyses for all pairs are reported in Table II. The correlations were positive between all pairs. The pairs with significant correlations ($p < 0.05$) included coupon failure strain and whole rib peak tensile strain, coupon failure stress and whole rib peak force, and coupon strain energy density and whole rib total energy. Significance was conserved across correlation analyses in that only the pairs that were found to be significantly correlated in the parametric analysis were also significant in the non-parametric analysis. Despite the presence of significant correlations between structural and material properties, the R^2 values were less than 0.5 for all comparisons (Table II), indicating that the material properties explained less than 50% of the variance in structural properties. The lowest R^2 value was observed for the modulus and stiffness ($R^2 = 0.0123$), while the highest value was observed for the strain energy density and total energy ($R^2 = 0.4424$). This demonstrated that the modulus explained approximately 1% of the variance in stiffness, while the strain energy density explained almost half of the variance in the total energy.

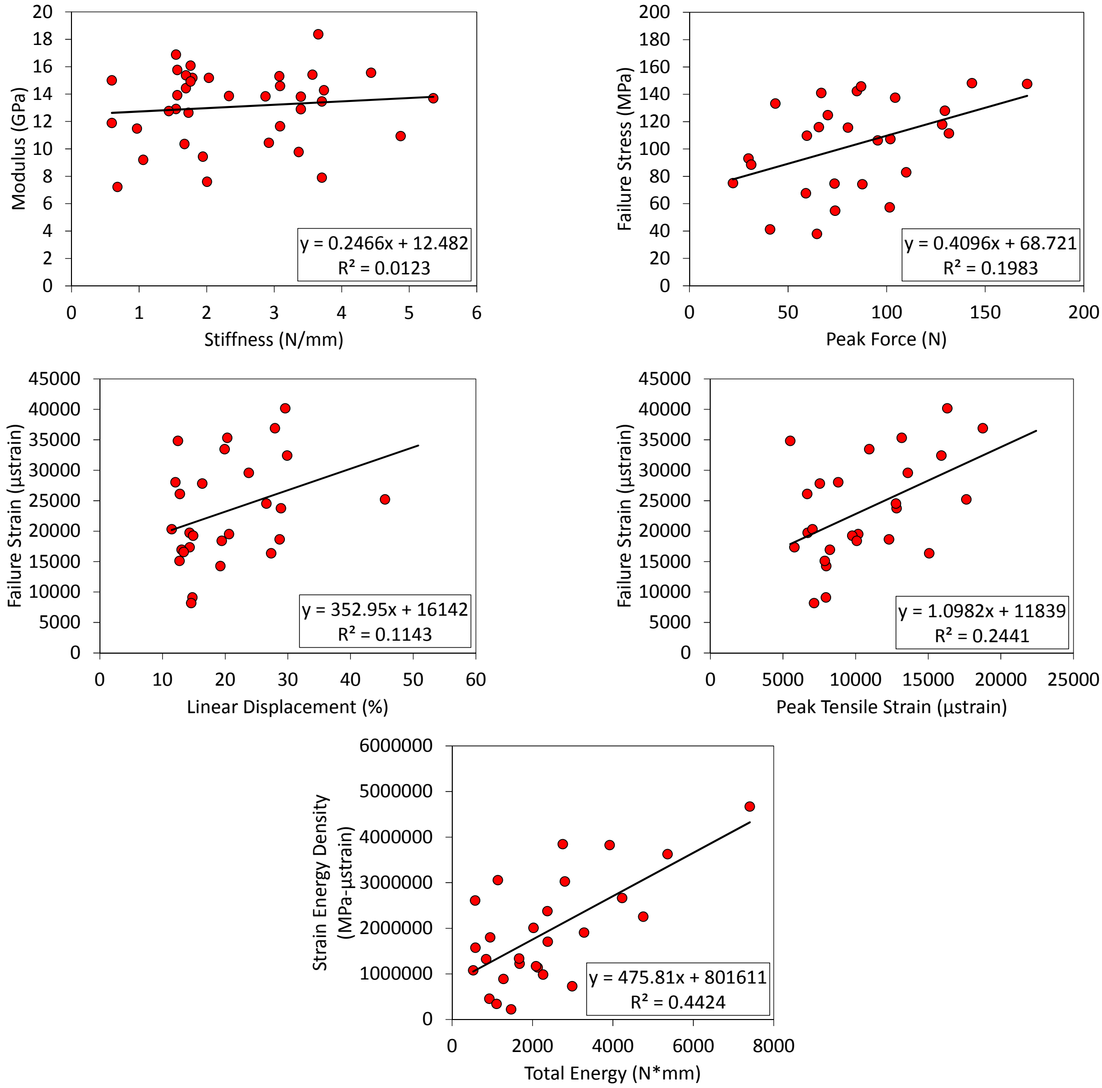

Fig. 5. Material properties from the coupon tests versus structural properties from the bending tests fit with a linear trend line.

TABLE I
MEAN MATERIAL AND STRUCTURAL PROPERTIES

Test Type	Property	Units	Mean	Standard Deviation
Tension Coupon	Modulus	GPa	13.08	2.69
	Failure Strain	μstrain	23262	8490
	Failure Stress	MPa	102.97	33.72
	Strain Energy Density	MPa-μstrain	1920373	1173718
Whole Rib Test	Stiffness	N/mm	2.52	1.28
	Linear Displacement	%	20.17	8.13
	Peak Tensile Strain	μstrain	10636	3847
	Peak Force	N	83.63	36.66
	Total Energy	N*mm	2351.26	1640.81

TABLE II

STATISTICAL CORRELATIONS FOR EACH MATERIAL PROPERTY/STRUCTURAL PROPERTY COMPARISON

Material Property	Structural Property	Pearson		Spearman		R^2
		r	p-value	ρ	p-value	
Modulus	Stiffness	0.1108	0.5137	0.0865	0.6109	0.0123
Failure Strain	Linear Displacement*	0.3381	0.0846	0.2985	0.1304	0.1143
Failure Strain	Peak Tensile Strain*	0.4941	**0.0103**	0.3990	**0.0435**	0.2441
Failure Stress	Peak Force	0.4453	**0.0199**	0.4292	**0.0255**	0.1983
Strain Energy Density	Total Energy*	0.6652	**0.0002**	0.5116	**0.0064**	0.4424

Note: An asterisk (*) indicates a structural property that was not normally distributed.
Bolded values indicate significance at $p < 0.05$.

IV. DISCUSSION

Three previous studies have quantified the tensile material properties of rib cortical bone at a similar strain rate as this study [7][17][19]. The same coupon fabrication and experimental setup were used in this study as in Kemper *et al.* [17] and Kemper *et al.* [7]. The average moduli, failure strains, and failure stresses (Table III) reported in these studies were comparable to the average values found in this study, with the averages from this study being slightly lower than the previous studies. These small differences can be attributed to between subject variation. Subit *et al.* [19] also conducted quasi-static tensile tests at a similar average strain rate (5.95 strain/s), but used a different fabrication and experimental setup than the current study. The average moduli and failure stresses were also comparable between the current study and Subit *et al*. However, the average failure strain reported by Subit *et al.* was lower than that found in this study and both studies by Kemper *et al*, indicating that less plastic deformation was observed by Subit *et al*. Possible reasons for this discrepancy has already been explored in [19]. Overall, the material properties found in this study were consistent with those previously reported for rib cortical bone.

TABLE III

COMPARISON TO MEAN MATERIAL PROPERTIES FROM PREVIOUS STUDIES

	Modulus GPa	Failure Strain µstrain	Failure Stress MPa	Number of Subjects
Current Study	13.1	23262	103.0	29
Kemper *et al.* [17]	13.9	26829	123.2	6
Kemper *et al*. [7]	14.4	25110	130.9	6
Subit *et al*. [19]	13.5	10600	112.1	3

The structural properties observed in this study were also consistent with those reported by previous studies that performed similar whole rib anterior/posterior bending tests (Table IV) [6][8][11][25]. The average structural properties of the current study were most similar to those reported by Charpail *et al.* and were least comparable to those reported by Schafman *et al.* However, it is important to note that linear stiffness was calculated differently by Charpail *et al.* and Kindig *et al*. and may not be directly comparable to the results of this study. Additionally, the tests conducted by Kindig *et al.* were performed under quasi-static conditions, whereas the tests performed by Charpail *et al.*, Schafman *et al.*, and the current study comprised dynamic impacts at 1 to 2 m/s. The differences between Schafman *et al.* and the current study may be attributed to between subject variation related to differences in sample demographics. Although both studies encompassed a wide range of ages, Schafman *et al.* included pediatric subjects whereas the current study did not. Furthermore, the number of males and females included in the current study is more balanced than in Schafman *et al.*, which included more male subjects.

TABLE IV
COMPARISON TO MEAN STRUCTURAL PROPERTIES FROM PREVIOUS STUDIES

	Stiffness N/mm	Linear Displacement %	Peak Force N	Number of Subjects
Current Study	2.42	20.17	83.63	29
Charpail *et al.* [8]	2.34	20.67	86.63	5
Kindig *et al*. [11]	2.31	33.04	60.67	3
Schafman *et al*. [25]	3.6	25.60	116.0	93

The positive correlations observed for all analogous pairs of structural and material properties indicates each material property had some influence on its corresponding structural property. A significant correlation was observed for all but two pairs: coupon modulus and whole rib stiffness, and coupon failure strain and whole rib linear displacement. This indicates that rib geometry may be contributing more to stiffness and linear displacement than the material properties. Strain energy density and total energy had the highest degree of correlation of all pairs. This is logical because energy absorption is primarily a function of the material. The low R^2 values observed for all comparisons indicated that the material properties did not explain the majority of the variance of the structural properties. This finding lends further support to the hypothesis that rib geometry has a strong influence on the structural properties.

Several studies have attempted to use modeling and theoretical approaches to gain insight into the mechanics of this simplified bending scenario with limited success. Charpail *et al*. [8] used a finite element model of three ribs that incorporated simplified rib-specific geometry, but constant material properties across all ribs, in an attempt to predict the fracture locations in the corresponding experimental tests based on the strains observed in the model. The model was able to approximately match the fracture locations, but was unable to match fracture timing. Charpail *et al.* concluded that discrepancies between the model and experiments were a result of the simplified rib geometry used for the model. Daegling *et al.* [27] performed similar bending tests on ribs instrumented with strain gages in order to study rib fracture mechanics. They used beam theory to predict the stresses occurring at the rib locations instrumented with strain gages and a non-specific elastic modulus to calculate "observed" stresses. Substantial differences between the observed and theoretical stresses were reported, and the authors attributed these differences to the assumption of elasticity and an oversimplification of rib geometry. Perz *et al.* [28] developed a finite element beam model using rib-specific geometry derived from CT data and non-specific material properties. The model was able to reasonably match the elastic portion of the force-deflection curves from bending tests based on geometric properties alone. However, their model limitations prevented additional analyses of plastic and failure behavior.

Charpail *et al*., Daegling *et al*., and Perz *et al*. demonstrated the importance of rib geometry on structural properties and mechanical behavior through modeling. Furthermore, a recent study by Murach *et al.* [29] showed that both cross-sectional and whole rib geometry explained a large amount of variance (35 – 75%) in rib structural response in the same bending scenario used in the current study. However, none of these studies attempted to account for rib-specific material properties in their models. The current study showed that rib material properties were only a partial contributor to the structural properties and that some material properties were more influential than others. The results of this study in conjunction with the literature empirically confirm the long-standing hypothesis that both material properties and rib geometry contribute to rib structural properties. This study is a first step toward a larger goal of quantifying the relative contributions of material properties and geometry on rib structural responses. Future analyses incorporating rib-specific cross-sectional and whole rib geometry will be performed as the necessary data are collected, and multivariate models will be constructed to understand the influence of all variables and their potential interactions. The data included in this study and future studies will provide a basis for improved modeling of rib mechanics and injury prediction.

A limitation of this study was the assumption that there was no difference in the structural and material properties between the left and right ribs. The results of previous research indicate that the assumption of left/right symmetry in rib material and structural properties is reasonable. Yoganandan and Pintar [14] tested this assumption with regard to structural properties using three-point bending tests, and found no difference in the modulus, force, and deflection between matched left and right ribs. Furthermore, Kemper *et al*. [7][17]

reported no significant within subject differences in material properties with respect to rib region or level on the same side of the rib cage. A logical extension of this finding is that no difference would be observed between the left and right sides of the rib cage.

Another limitation of this study was that the data analysis for the bending tests assumed that all motion was relegated to one plane and the ribs only experienced bending. However, some out of plane motion is possible and could result in torsion and shear loading. Structural properties derived from shear loading would not be directly comparable to the tensile material properties derived from the coupon tests.

Finally, this study assumed that rib cortical bone is a homogenous material despite its true nature as a composite material. The microstructure of bone is known to influence the macroscale material properties. Increases in intracortical porosity and number of secondary osteons have been shown to decrease material properties [30-35]. Some studies have reported that the degree of mineralization influences bone material properties [31][33]. However, this link was not observed in all studies [17][32][36][37]. Variation in cortical bone microstructure along the length of the rib may have influenced the structural and material properties reported in this study. However, as noted above, Kemper *et al.* [7][17] found in two previous studies that tensile material properties did not significantly vary along the length of the rib so any impact of microstructural variation on material property variation within a rib is likely small. Variation in rib microstructural organization and composition between individuals has been established in prior studies specific to the rib [38][39], and likely contributed to the inter-subject variation in material and structural properties observed in this study. Therefore, future work will investigate the influence of cortical bone microstructure on rib material and structural properties. Additionally, the effect of age and sex on the relationship between the material and structural properties should be assessed on a larger and more inclusive sample as microstructural changes are thought to influence age and sex differences.

V. Conclusions

Positive correlations were observed for all pairs of structural and material properties. Coupon strain energy density and whole rib total energy had the highest correlation, while coupon modulus and whole rib stiffness had the lowest correlation. The structural properties with significant correlations (peak tensile strain, peak force, and strain energy density) were more influenced by material properties compared to the structural properties without significant correlations (linear displacement and stiffness). All comparisons resulted in R^2 values below 0.5, indicating the material properties did not explain the majority of the variance of the structural properties. Given that the structural response is dependent on both the material and geometric properties, this finding lends further support to the hypothesis that local and global rib geometries likely have a strong influence on the structural properties. This study is the first step in determining the relative contributions of material properties and geometry on the structural response of whole ribs, which will provide a basis for improved modeling of rib mechanics. Elucidating the influences of these variables on the structural response of the rib will provide insight into the sources of thoracic injury tolerance variability between different populations.

VI. Acknowledgement

The authors would like to thank Autoliv for sponsoring this research and the National Highway Traffic Safety Administration for use of their equipment. The opinions expressed in the manuscript are solely those of the authors and do not represent the views of any sponsor. Thank you to Michelle Murach, John Bolte IV, Arrianna Willis, and David Stark of the Injury Biomechanics Research Center. Finally, thank you to the anatomical donors whose generous gifts make this research possible.

VII. References

[1] Cavanaugh, J.M. and Yoganandan, N., "Accidental Injury Biomechanics and Prevention", pages 331-372, Springer: New York, 2015

[2] Galan, G., Pe alver, J., et al. Blunt chest injuries in 1696 patients. *European journal of cardio-thoracic surgery*, 1992. 6(6): p. 284-287

[3] Kent, R. and Patrie, J. Chest deflection tolerance to blunt anterior loading is sensitive to age but not load distribution. *Forensic science international*, 2005. 149(2): p. 121-128

[4] Kent, R., Sang-Hyun, L., Darvish, K., and Wang, S. Structural and material changes in the aging thorax and their role in crash protection for older occupants. *Stapp car Crash journal*, 2005. 49: p. 231-249
[5] Zhou, Q., Rouhana, S.W., and Melvin, J.W. Age effects on thoracic injury tolerance. *Proceedings of 40th Stapp Car Crash Conference*, 1996. Albuquerque, NM
[6] Agnew, A.M., Schafman, M., Moorhouse, K., White, S.E., and Kang, Y.-S. The effect of age on the structural properties of human ribs. *Journal of the mechanical behavior of biomedical materials*, 2015. 41: p. 302-314
[7] Kemper, A.R., McNally, C., et al. The biomechanics of human ribs: material and structural properties from dynamic tension and bending tests. *Stapp Car Crash Journal*, 2007. 51: p. 235-273
[8] Charpail, E., Trosseille, X., Petit, P., and Laporte, S. Characterization of PMHS ribs: a new test methodology. *Stapp car crash journal*, 2005. 49: p. 183-198
[9] Cormier, J.M., Stitzel, J.D., Duma, S.M., and Matsuoka, F. Regional variation in the structural response and geometrical properties of human ribs. *Proceedings of Annual Proceedings/Association for the Advancement of Automotive Medicine*, 2005.
[10] Granik, G. and Stein, I. Human ribs: static testing as a promising medical application. *Journal of Biomechanics*, 1973. 6(3): p. 237-240
[11] Kindig, M., Lau, A.G., and Kent, R.W. Biomechanical response of ribs under quasistatic frontal loading. *Traffic injury prevention*, 2011. 12(4): p. 377-387
[12] Sacreste, J., Brun-Cassan, F., et al. Proposal for a thorax tolerance level in side impacts based on 62 tests performed with cadavers having known bone condition. *Proceedings of 26th Stapp Car Crash Conference*, 1982.
[13] Stein, I. and Granik, G. Rib structure and bending strength: an autopsy study. *Calcified Tissue International*, 1976. 20(1): p. 61-73
[14] Yoganandan, N. and Pintar, F. Biomechanics of human thoracic ribs. *Transactions-American Society of Mechanical Engineers Journal of Biomechanical Engineering*, 1998. 120: p. 100-105
[15] Kalra, A., Saif, T., et al. Characterization of Human Rib Biomechanical Responses due to Three-Point Bending. *Stapp car crash journal*, 2015. 59: p. 113-130
[16] Tomasch, E., Kirschbichler, S., et al. Methodology to predict thresholds for loading corridors of human ribs. *Proceedings of International Research Council on the Biomechanics of Injury Conference*, 2010. Hanover, Germany
[17] Kemper, A.R., McNally, C., et al. Material properties of human rib cortical bone from dynamic tension coupon testing. *Stapp Car Crash J*, 2005. 49(11): p. 199-230
[18] Stitzel, J.D., Cormier, J.M., Barretta, J.T., and Kennedy, E.A. Defining regional variation in the material properties of human rib cortical bone and its effect on fracture prediction. *Stapp car crash journal*, 2003. 47: p. 243-265
[19] Subit, D., de Dios, E.d.P., Valazquez-Ameijide, J., Arregui-Dalmases, C., and Crandall, J. Tensile material properties of human rib cortical bone under quasi-static and dynamic failure loading and influence of the bone microstucture on failure characteristics. 2011. https://arxiv.org/abs/1108.0390.
[20] Borchers, R.E., Gibson, L.J., Burchardt, H., and Hayes, W.C. Effects of selected thermal variables on the mechanical properties of trabecular bone. *Biomaterials*, 1995. 16(7): p. 545-551
[21] Hamer, A., Strachan, J., et al. Biomechanical properties of cortical allograft bone using a new method of bone strength measurement. *Bone & Joint Journal*, 1996. 78(3): p. 363-368
[22] Linde, F. and Sørensen, H.C.F. The effect of different storage methods on the mechanical properties of trabecular bone. *Journal of biomechanics*, 1993. 26(10): p. 1249-1252
[23] Panjabi, M.M., Krag, M., Summers, D., and Videman, T. Biomechanical time-tolerance of fresh cadaveric human spine specimens. *Journal of Orthopaedic Research*, 1985. 3(3): p. 292-300
[24] Pelker, R.R., Friedlaender, G.E., Markham, T.C., Panjabi, M.M., and Moen, C.J. Effects of freezing and freeze-drying on the biomechanical properties of rat bone. *Journal of Orthopaedic Research*, 1983. 1(4): p. 405-411
[25] Schafman, M.A., Kang, Y.-S., et al. Age and sex alone are insufficient to predict human rib structural response to dynamic AP loading. *Journal of Biomechanics*, 2016. 49(14): p. 3516-3522
[26] SAE. Instrumentation for Impact Test. 1995, Society of Automotive Engineers: Warrendale, PA.
[27] Daegling, D.J., Warren, M.W., Hotzman, J.L., and Self, C.J. Structural analysis of human rib fracture and implications for forensic interpretation. *Journal of forensic sciences*, 2008. 53(6): p. 1301-1307

[28] Perz, R., Toczyski, J., et al. Evaluation of the geometrical properties distribution along the human ribs using different X-Ray imaging methods. *Proceedings of International Research Council on the Biomechanics of Injury Conference*, 2013. Gothenburg, Sweden

[29] Murach, M.M., Kang, Y.-S., et al. Rib Geometry Explains Variation in Dynamic Structural Response: Potential Implications for Frontal Impact Fracture Risk. *Annals of Biomedical Engineering*, 2017: p. 1-15

[30] Currey, J. Differences in the tensile strength of bone of different histological types. *Journal of anatomy*, 1959. 93(Pt 1): p. 87-95

[31] Currey, J.D. The effect of porosity and mineral content on the Young's modulus of elasticity of compact bone. *Journal of biomechanics*, 1988. 21(2): p. 131-139

[32] Mccalden, R.W., McGeough, J.A., and Barker, M.B. Age-related changes in the tensile properties of cortical bone. The relative importance of changes in porosity, mineralization, and microstructure. *J Bone Joint Surg Am*, 1993. 75(8): p. 1193-1205

[33] Schaffler, M.B. and Burr, D.B. Stiffness of compact bone: effects of porosity and density. *Journal of biomechanics*, 1988. 21(1): p. 13-16

[34] Vincentelli, R. and Grigoroy, M. The effect of Haversian remodeling on the tensile properties of human cortical bone. *Journal of biomechanics*, 1985. 18(3): p. 201-207

[35] Zioupos, P. Ageing human bone: factors affecting its biomechanical properties and the role of collagen. *Journal of Biomaterials Applications*, 2001. 15(3): p. 187-229

[36] Mueller, K.H., Trias, A., and Ray, R.D. Bone Density and Composition: Age-related and pathological changes in water and mineral content. *Journal of Bone & Joint Surgery - American Volume*, 1966. 48(1): p. 140-148

[37] Yeni, Y., Brown, C., and Norman, T.L. Influence of bone composition and apparent density on fracture toughness of the human femur and tibia. *Bone*, 1998. 22(1): p. 79-84

[38] Agnew, A.M., Dominguez, V.M., Sciulli, P.W., and Stout, S.D. Variability of in vivo linear microcrack accumulation in the cortex of elderly human ribs. *Bone reports*, 2017. 6: p. 60-63

[39] Agnew, A.M. and Stout, S.D. Brief communication: reevaluating osteoporosis in human ribs: the role of intracortical porosity. *American journal of physical anthropology*, 2012. 148(3): p. 462-466